Proceedings World Geothermal Congress 2026
Calgary, Canada, June 8 – 11, 2026

Sources of helium and associated heat of in hydrothermal fluids from the central western branch of the East African Rift System (Democratic Republic of Congo and Burundi)

Wisdom K. Kavyavu[1,2,3]*, Daniele. L. Pinti[1], Bienfait. K. Simisi[3,4], Dario Tedesco[5,6]

[1] Geotop & Département des sciences de la Terre et de l'atmosphère, Université de Québec à Montréal, H2X 3Y7 Canada, [2] Département de Géologie, Université de Goma, DRC,[3] Comité de Pilotage et de Développement des Ressources Géothermales, Goma, DRC, [4] Département de Géologie, Université de la Conservation de la Nature et Développement de Kasugho, Nord Kivu, DRC, [5] Department of Environmental, Biological and Pharmaceutical Sciences and Technologies, Università dela Campania "Luigi Vanvitelli", Caserta, Italy, [6] Mission de l'Organisation des Nations Unies pour la Stabilisation en RDC (MONUSCO), DRC

* To whom correspondence must be sent: wisdomkambale@gmail.com

Keywords: Ruzizi basin, Geothermal Fields, East Africa rift, Noble Gases isotopes

0. SUMMARY

The Lake Kivu bassin, central western branch of the East African rift system, has numerous hot springs expressing heat at depth. The chemistry and isotopic signatures of hydrothermal fluids are known along the northern shore of Lake Kivu, monitoring the Nyiragongo volcano. However, the southern shore of Lake Kivu, down to Tanganyika Lake, a non-volcanic area, has been ignored while there are tens of hydrothermal manifestations. This study fills the gap by sampling 15 hot springs, two volcanic lakes, and three cold springs on the border of DRC and Burundi. Stable isotopes of water (δ^2H and $\delta^{18}O$), noble gases He ($^3He/^4He$), Ne, and Ar, Sr isotopes ($^{87}Sr/^{86}Sr$), with major and trace elements were analyzed. Several samples are Na+K- HCO3 and HCO3-Mg+Ca and are Immature type. The stable isotopes plot shows a meteoric in origin, only the lake waters are fractionationed by evaporation. Helium ($^3He/^4He$) ratios are normalized and corrected for the atmospheric component (Rc/Ra) range from 0.056 to 1.987, suggesting a mixing of crustal source and about 13% of mantle helium. The $^{87}Sr/^{86}Sr$ ratios range from 0.7036 (Lac Vert) volcanic to 0.77173 in hot springs, radiogenic value likely indicating water-rock interaction with silicate minerals. These results contrast with those on northern shore of Lake Kivu characterized by magmatic helium, thus, indicating that heat controls the volcanoes and the local geothermal gradient facilitated by the extensional faults. Small magmatic helium observed in some samples is possibly related to the leaching of local intrusions rather than addition from magma melts at depth.

1. INTRODUCTION

1.1 Aims:

(i) Estimation of the contribution of surface water to the hydrothermal system using stable water isotopes $^2H/^1H$ (δ^2H) and $^{18}O/^{16}O$ ($\delta^{18}O$).

(ii) Identification of the origins of heat in thermal waters. Inferred from the temperature, the heat may be the result of the regional geothermal gradient or of a magmatic intrusion confined in the subsurface.

(iii) Quantification and identification of the origins (mantle, atmospheric, and crustal) of helium in thermal springs. This aspect is determined by helium isotopic ratio ($^3He/^4He$), which provides information on the origin of the fluids and the possible source of associated heat.

(iv) Quantification of water-rock interactions to verify whether the fluids have reached equilibrium with the minerals in the reservoir rocks. The Sr isotopic ratios ($^{87}Sr/^{86}Sr$) were better identifier of the crustal processes occurring in the reservoir.

The Kivu -Tanganyika rifts (KTR hereafter) are the central section of the western branch of the East Africa Rift System (WBEARS hereafter) between two active volcanic provinces, the Virunga in the north and the Rukwa in the south. These two volcano fields have high-enthalpy geothermal systems whose lateral extension is still unknown. Geothermal resources in this highly populated region could make a significant contribution to human daily needs and help shifting from fossil fuels to green energy sources. However, these must be appropriately evaluated for possible future exploitation, which is the primary focus of this study.

Chemically inert, noble gases, He, Ne, Ar, Kr, and Xe are widely used to determine hydrothermal fluids' sources, particularly helium isotopes ($^3He/^4He$) (e.g, Kennedy and Truesdell, 1996, Pinti et al., 2013, Tedesco et al., 2010). Helium in fluids can be derived from the atmosphere by dissolution into groundwater at the recharge area (Air-saturated or ASW conditions), from the mantle by advection from magma intrusions to the hydrothermal convective system (e.g.,

Han et al., 2022); from the crust by radioactive decay of U and Th contained in rocks (e.g., Kulongoski and Hilton, 2011).

These three terrestrial reservoirs have a distinct $^{3}He/^{4}He$ ratio (or R). This ratio, normalized to that of the atmosphere ($Ra = 1.384 \times 10^{-6}$) or R/Ra is of 8±1 for the Depleted MORB-type mantle (or DMM; Allègre et al., 1995), i.e. is enriched in primordial ^{3}He compared to ^{4}He and respect to the atmosphere. This ratio equals 0.02 for the crust, resulting from the dominant production of radiogenic ^{4}He from a-decay of U and Th in rocks and a minor amount of ^{3}He from nuclear reactions with ^{6}Li (Ballentine and Burnard, 2002). Finally, the atmospheric ratio in dissolved water is 0.983. Thus, the $^{3}He/^{4}He$ ratio can help identify the presence of meteoric water, fossil water enriched in crustal helium (e.g., Pinti et al., 2019), and mantle-derived fluids. In high-enthalpy geothermal reservoirs with little meteoric recharge or high mantle fluxes as in hotspot regions (e.g., Roulleau et al., 2025), fluids can also have preserved terrigenic Ne and Ar of crustal and/or mantle origin. The majority of hydrothermal fluid studies in the WBEARS are concentrated around the VVP (Tedesco et al., 2010) and, more recently in the RuVP southwestern Tanzania(Kimani et al., 2021).

1.2 Sampling and analytical methods :

In May 2024, fifteen thermal springs were collected across the D.R. Congo and Burundi, 2 rift-lakes (Kivu and Tanganyika), 2 volcano crater lakes (Lac Vert and Lac Noir) on the flank of the Nyirangogo volcano, and the White Nile River source in Burundi.

The temperatures of the springs, sources, and lakes were taken using a portable HH74K digital thermometer ranging from -100 to 850°C with a precision of 0.1˚C. The pH and conductivity (in msm/cm^{3}) were measured using a HI98129-HI98230 waterproof, portable multiparameter probe. Samples were collected in 8 ml Nalgene bottles for major and trace ions and in 8 ml bottles for stable water isotopes. Samples for strontium isotopic analyses were collected in 250 ml Nalgene bottles without chemical treatment. Noble gases were collected in 14 cm^{3} volume refrigeration-grade copper tubes with a diameter of 3/8 inches. To prevent air contamination, samples were taken using a water displacement method (e.g., Poblete-Gonzales et al., 2025). The $\delta^{2}H$-H_2O analysis was performed on 200 ml pipetted in a 3 ml vial, closed with a septum cap and transferred to a 40°C heated rack. For $\delta^{2}H$ a hydrophobic platinum catalyst (Hokko beads) was added. After 1 hour, air in the vials was replaced with CO_2 (for $\delta^{18}O$) or H_2 (for $\delta^{2}H$) using the AquaPrep. Three internal standard waters ($\delta^{18}O$=0.82±0.04 ‰, -14.40±0.04 ‰ & -25.73±0.03 ‰; $\delta^{2}H$=5.51±0.54 ‰, -102.29±0.44 ‰ & -184.94±0.79 ‰) were used to normalize the results on the VSMOW scale (VSMOW2-SLAP2). A 4th standard water ($\delta^{18}O$=-7.22±0.03 ‰; $\delta^{2}H$=-52.82±0.93 ‰) was analyzed as an unknown to assess the exactness of the normalization. The overall analytical uncertainty (1s) is better than ±0.1 ‰ for $\delta^{18}O$ and ±2.0 ‰ for $\delta^{2}H$. These uncertainties are based on the propagation of uncertainties of the normalization of the internal reference materials and the samples but do not include the homogeneity nor the representativity of the sample. Results are given in delta units (δ) in ‰ vs VSMOW.

The $^{87}Sr/^{86}Sr$ isotopic composition was analyzed on a NU Instruments® Plasma 3 MC-ICP-MS. Classic Sr-resin (Eichrom, Lisle, IL, USA) ion chromatography (double-pass) was used to ensure the purification of the Sr from potential Rb isobaric interference. All the reagents were double distilled within class 100 enclosures in DST-1000 sub-boiling stills (Savillex) and were diluted with Milli-Q ultrapure water (Millipore Sigma). The measurements were processed on the Plasma 3 and an Aridus II dissolved the membrane (Teledyne CETAC technologies). ‘‘On-peak-zero’’ gas blank measurements were carried out to account for imperfect small residual washout and krypton interferences (coming from the plasma argon gas supply; Praxair). The mass bias was corrected by normalizing to $^{86}Sr/^{88}Sr = 0.1194$. The NBS987 Sr standard was measured during the analytical sessions and yielded an $^{87}Sr/^{86}Sr$ ratio of 0.71024 ± 0.00002.

For noble gas analyses, sealed copper tubes within hot spring water were extracted for separating gas trapping in a stainless steel 12.5 cc finger closed with a Swagelok below valve. The finger was then connected to the purification line with two Ti-getters at 600°C for 15 min and 10 min at ambient temperature, and one SAES ST-707 getter at 125°C for 15 min, 10 min at ambient temperature. Purified gases were then sent on Advanced Research System (ARS) cryogenic traps containing activated charcoal at 12K and released sequentially at 40K (He), 90K (Ne) and 220 K (Ar). Noble gases were measured on a multi-collection noble mass spectrometer Thermo® Helix-MC. The ^{3}He was measured by ion counting on the axial Compact Discrete Dynode (CDD) detector. The ^{4}He and other noble gas isotopes (Ne, Ar) were measured using the axial Faraday. Typical static blanks for the Helix and the purification line are not measurable for ^{3}He on the CDD, while on the faraday, they are as follows: 1fA on ^{4}He; 1fA on ^{20}Ne; 5 fA on ^{40}Ar. Signals were calibrated against a known aliquot of standard air. The ^{20}Ne was measured on the axial Faraday but the resolution is sufficient to measure it on the shoulder of $^{40}Ar^{++}$. A test measuring ^{20}Ne on the high-resolution (L1) Faraday shows the same $^{20}Ne/^{22}Ne$ ratio measured on the axial Faraday within uncertainties, indicating that the shoulder plateau is unaffected by the $^{40}Ar^{++}$. The CO_2 (mass 44) measured during standard does not produce resolvable interferences on mass 22. Typical standard reproducibility for ^{4}He and ^{22}Ne contents was 2-5% (based on 1-month standard

measurements). Errors on the $^{3}He/^{4}He$ ratios were about 2% at 1s. Abundances of ^{4}He, ^{20}Ne, and ^{36}Ar are expressed as cm^3STP^*/g_{H2O} (*Standard Temperature and Pressure). Measured R/Ra ratios were corrected for the atmospheric component (Rc/Ra) by using the $^{4}He/^{20}Ne$ ratio, based on the equation (Craig et al., 1978):

$$(Rc/Ra) = [(R/Ra)_{meas}-r]/(1-r) \quad (1)$$

$$r = (^{4}He/^{20}Ne)_{ASW} / ^{4}He/^{20}Ne)_{meas} \quad (2)$$

with $(R/Ra)_{meas}$ the measured helium isotopic ratio, $(^{4}He/^{20}Ne)_{ASW}$ the ratio corresponding to Air Saturated Water at 21˚C (Mean Annual Air Temperature or MAAT at Goma, RDC), and $(^{4}He/^{20}Ne)_{meas}$ the measured ratio in the water sample.

1.3. Previous works:

There are several scientific and professional documents reporting applied isotopic geochemistry of waters in the Kivu and Tanganyika Rift (KTR) and precisely three of them analyzed noble gases of hosted by the KTR. Tedesco et al. (2010) onto volcano monitoring and Bärenbold et al. (2020) studied the maturity level of methane of the Kivu Lake while recently Boudoire et al. (2022) magmatic displacement under floor of Goma city respectively.

1.4. Geothermal settings of the KTR:

The geothermal activity around the KTR can be classified into three types based on the topography and local geology:

a) Geothermal springs on lacustrine shorelines: around the Kivu and Tanganyika Lakes, cold and hot springs occur on the shores or within 1000m from the lakes.

b) Geothermal springs located in the Ruzizi basin: the medium slope is a heat flow rising between the two Rift-lakes. Generally, later sedimentary deposits cover earlier magmatic rocks with rapid flow rates and high temperatures of 66-70°C for Ruhwa, Katogota, and Uvira (Kamvivira).

c) Geothermal springs out of the rift: some are hosted within the stanniferous belt in Congo (Kisuma, Kichula), isolated volcanic lavas in Kamitunga with Twangingiza geothermal group (Bugoyi and Luidja hot springs) (Walemba, 2001) and Walikale. Others are in faulted metamorphic facies, such as Muyange, Muhweza controlled by brecciated schist in Bururi close to Nickeliferous lateritic trend in Burundi (Bandyayera, 1997).

In these three groups, travertine formation is present, reaching at least 1m above ground level around the outlet of the resurgences.

2. RESULTS

The water temperature of thermal springs ranges from 32° to 67°C for thermal springs and the pH ranges from very acidic (e.g. : 3.1 for spring Ruhagarika) to alkaline (9). The lowest is less than that reported in the literature of 5 in the region (Tedesco et al., 2010), and it may derive from incorrect manipulation during field measurement. The electric conductivity ranges from 10 µS/cm to 3745.

From the Piper diagram, the waters are of two main families: Ca-Mg-HCO_3 type (mainly springs in Buriri and South Kivu) and Na-K-HCO_3 in Tanganyika and Ruzizi (annex 3). The $\delta^{2}H$ and $\delta^{18}O$ values of the hot springs vary from -4.81‰ to -2.70‰ and -22.2‰ to -5.8‰ vs. V-SMOW, respectively, except for the spring Pemba (annex 1). This latter sample shows much heavier values of +3.26‰ and +22.9‰ vs. V-SMOW in the range of those measured in surface lake water and caused by evaporation. The $^{87}Sr/^{86}Sr$ ratios (Table 2) range from 0.70326±0.00001 for lake water from Lac Vert to 0.77520±0.00001 for thermal spring Uvira (UV-01) in the Ruzizi region. The ^{4}He concentration varies from 2.0 x 10^{-8} to 6.21 x 10^{-4} cm^3STP/g, the lowest values are recorded in lakes, and the highest are from hot springs in the Ruzizi basin (annex 5). The $^{3}He/^{4}He$ ratios normalized to the atmospheric ratio or R/Ra range from 0.058±0.002 to 1.304±0.04. The atmospheric ratios corrected of the atmospheric component or Rc/Ra range from 0.056±0.002 to 1.904±0.62. The ^{20}Ne concentrations range from 1.49 x 10^{-8} to 2.99 x 10^{-6} cm^3STP/g while ^{36}Ar concentrations range from 1.31 x 10^{-7} to 1.48 x $10^{-5}cm^3STP/g$. The Ne isotopic ratios $^{20}Ne/^{22}Ne$ and $^{21}Ne/^{22}Ne$ range from nearly atmospheric values (9.80 and 0.0290; to 11.43 and 0.0312. The Ar isotopic ratios $^{40}Ar/^{36}Ar$ and $^{38}Ar/^{36}Ar$ range from 288.1 to 320.8 and from 0.1845 to 0.1931.

Finally, the $^{87}Sr/^{86}Sr$ ratios range from 0.7036±0.0001 to 0.7752±0.0001, the lowest is of the Lake Kivu reflecting efforts of local basalts rocks from Nyiragongo (0.7045–0.7047) (e.g., Chakrabarti et al., 2009) while the highest related on the local felsic magmatic rocks indicating a very radiogenic Sr reservoir such as the values in muds from the Kivu and Tanganyika region and those weathered from the Proterozoic basement granitoid (Garzanti et al., 2013).

Figure 1 shows Craig's plot $^{4}He/^{20}Ne$ vs measured R/Ra of the sampled waters and existent data reported from Tedesco et al. (2010) on the springs and fumaroles from the Nyiragongo volcano summit and on the Lake Kivu shores, helium isotopic ratios measured in recent fissures within the town of Goma (RDC) and Gisenyi (Rwanda) and reports ranging

from 0.47 to 0.77 Ra (Boudoire et al., 2022) were not reported in figure 1. Data from this study (colored dots) are reported following the same color schema as in annex 3. We reported the endmembers of the MORB-type Depleted Mantle (labelled DMM with R/Ra of 8 and $^{4}He/^{20}Ne$ of 1000; the crust (with R/Ra of 0.02 and $^{4}He/^{20}Ne$ of 1000, and the atmospheric component dissolved at the recharge of the meteoric water (ASW or Air Saturated Water). The R/Ra value of the ASW endmember is assumed to be slightly fractionated air (0.983) and a $^{4}He/^{20}Ne$ of 0.269 calculated at the MAAT (Mean Annual Air Temperature) of 21˚C using noble gas solubility data from Smith S.P and Kennedy B.M (1983). Gray lines indicate the mixing line between ASW, and a mantle component diluted progressively by crustal helium.

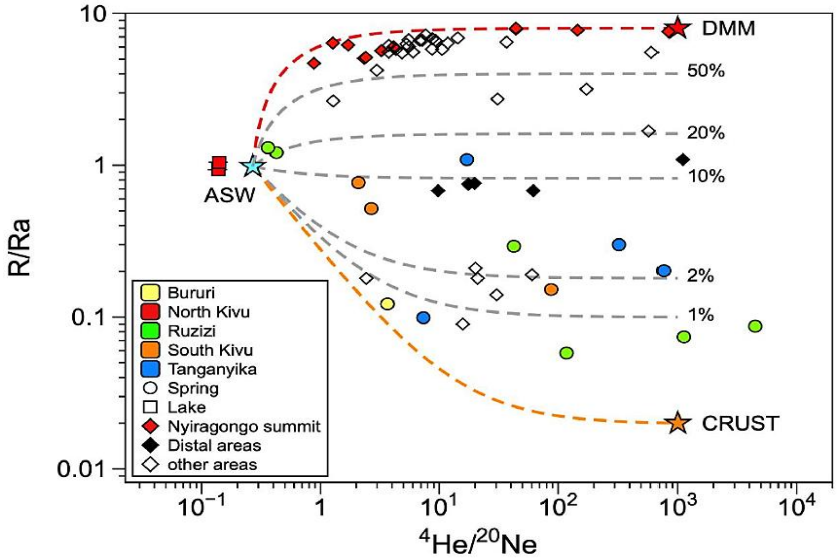


Figure 1. The $^{4}He/^{20}Ne$ ratio vs R/Ra of the sampled spring and lake waters. Data from this study and Tedesco et al. (2010). The diamond filled with red is the fumarole of Nyiragongo, the whitish one is the Mazuku, the black one is a thermal spring.

It appears that thermal springs from the southern areas of Kivu down to the Tanganyika contain a maximum mantle helium proportion of less than 8% measured in sample CIB-01 (Cibitoke) and MHKa-01 (Katana). Pemba, which shows a stable isotopic composition of lake water (annex 1), shows the highest proportion of mantle helium of 13.1%. To reconcile these contrasting results, we must assume that the gas phase containing mantle helium is decoupled from the water flow, which is mainly sourced by lake water from the near Tanganyika shore. The small amount of mantle helium observed in sampled thermal waters could be a fossil one exchanged with Cenozoic (21 to 2.6 Ma old) volcanic rocks (Pouclet et al., 2016) (magma aging; e.g., Kennedy & Van Soest, 2006). Older intrusions are of Neoproterozoic ages (Pouclet et al., 2016) and the mantle helium has likely been completely diluted by radiogenic ^{4}He beyond recognition (e.g., Torgersen et al., 1995).

3. CONCLUSIONS

The results show that moving south of the Nyiragongo volcanic to the southern shore of Lake Kivu, the thermal waters contain little helium of mantle origin (less than 13% in volume), and most gases are of crustal origin. The relationship between the $^{87}Sr/^{86}Sr$ ratios and the helium and argon isotopic ratios suggests that these fluids have reached considerable depths to interact with Precambrian African basement rocks and likely reached temperatures up to 200-300˚C, corresponding to the closure temperature of argon for most silicate minerals. This seems confirmed by reservoir temperature estimation based on Na-K-Mg geothermometers. Most of the sampled springs are along faults bordering the WBEARS.

4. AKNOWLEDGEMENTS

Warm thanks to Congolese and Burundian Geothermal energy committees for collaborative implication in planning the field works, to Camila Paz Poblete Gonzalez (Un. Concéption, Chile) and Isabel Martinez (UNAM, Mexico) for discussions. This research project has been supported financially by the NSERC Discovery Grant (RGPIN-2015-05378) to DLP and an exemption scholarship from the Embassy of the Democratic Republic of Congo in Canada to WKK. We acknowledge Fonds de recherche du Québec - Nature et technologies (FRQNT - Grant 2018RS-203300) to Geotop.

5. REFERENCES

Allègre, C.J., Moreira, M., Staudacher, T., 1995. $^{4}He/^{3}He$ dispersion and mantle convection. Geophys. Res. Lett. 22, 2325-2328. https://doi.org/10.1029/95GL02307

Ballentine, C.J., Burnard, P.G., 2002. Production, release and transport of noble gases in the continental crust. Rev. Mineral. Geochem. 47, 481-538.

Bandyayera, D. (1997). Formation des latérites nickélifères et mode de distribution des éléments du groupe du platine dans les profils latéritiques du complexe de Musongati, Burundi /. Université du Québec à Chicoutimi. https://doi.org/10.1522/1531842

Bärenbold, F., Schmid, M., Brennwald, M. S., & Kipfer, R. (2020). Missing atmospheric noble gases in a large, tropical lake : The case of Lake Kivu, East-Africa. Chemical Geology, 532, 119374. https://doi.org/10.1016/j.chemgeo.2019.119374

Boudoire, G., Calabrese, S., Colacicco, A., Sordini, P., Habakaramo Macumu, P., Rafflin, V., Valade, S., Mweze, T., Kazadi Mwepu, J.-C., Safari Habari, F., Amani Kahamire, T., Mumbere Mutima, Y., Ngaruye, J.-C., Tuyishime, A., Tumaini Sadiki, A., Mavonga Tuluka, G., Mapendano Yalire, M., Kets, E.-D., Grassa, F., … Tedesco, D. (2022). Scientific response to the 2021 eruption of Nyiragongo based on the implementation of a participatory monitoring system. Scientific Reports, 12(1), 7488. https://doi.org/10.1038/s41598-022-11149-0

Chakrabarti, R., Basu, A.R., Santo, A.P., Tedesco, D., Vaselli, O., 2009. Isotopic and geochemical evidence for a heterogeneous mantle plume origin of the Virunga volcanics, Western rift, East African Rift system. Chem. Geol. 259, 273-289. https://doi.org/10.1016/j.chemgeo.2008.11.010

Garzanti, E., Padoan, M., Setti, M., Najman, Y., Peruta, L., & Villa, I. M. (2013). Weathering geochemistry and Sr-Nd fingerprints of equatorial upper Nile and Congo muds. Geochemistry, Geophysics, Geosystems, 14(2), 292-316. https://doi.org/10.1002/ggge.20060

Han, G., Pinti, D.L., Castro, M.C., Hernández-Hernández, M.A., Lopez-Hernández, A., Hall, C.M., Zheng, G., Ramírez-Montes, M., 2022. Heat, noble gases and CO_2 sources in geothermal fields of Mexico. Appl. Geochem. 144. https://doi.org/10.1016/j.apgeochem.2022.105391.105391

Kasay, G. M., Bolarinwa, A. T., Aromolaran, O. K., Nzolang, C., & Mambo, V. S. (2021). A review of the geological settings, ages and economic potentials of carbonatites in the Democratic Republic of Congo. Applied Earth Science, 130(3), 143-160. https://doi.org/10.1080/25726838.2021.1911585

Kennedy, B. M., & Van Soest, M. C. 2006. A helium isotope perspective on the Dixie Valley, Nevada, hydrothermal system. Geothermics, 35(1), 26-43. https://doi.org/10.1016/j.geothermics.2005.09.004

Kimani, C. N., Kasanzu, C. H., Tyne, R. L., Mtili, K. M., Byrne, D. J., Kazimoto, E. O., Hillegonds, D. J., Ballentine, C. J., & Barry, P. H. (2021). He, Ne, Ar and CO2 systematics of the Rungwe Volcanic Province, Tanzania : Implications for fluid source and dynamics. Chemical Geology, 586, 120584. https://doi.org/10.1016/j.chemgeo.2021.120584

Kulongoski, J.T., Hilton, D.R., 2011. Applications of Groundwater Helium, Handbook of Environmental Isotope Geochemistry, Volume 1. Springer Isotope Handbook, Reston, VA, pp. 285-304. https://doi.org/10.1007/978-3-642-10637-8_15

Pinti, D.L., Castro, M.C., López-Hernández, A., Hernández Hernández, M.A., Richard, L., Hall, C.M., Shouakar-Stash, O., Flores-Armenta, M., Rodríguez-Rodríguez, M.H., 2019. Cerro Prieto Geothermal Field (Baja California, Mexico) – A fossil system? Insights from a noble gas study. J. Volcanol. Geother. Res. 371, 32-45. https://doi.org/10.1016/j.jvolgeores.2018.12.010

Pinti, D.L., Castro, M.C., Shouakar-Stash, O., Tremblay, A., Garduño, V.H., Hall, C.M., Hélie, J.F., Ghaleb, B., 2013. Evolution of the geothermal fluids at Los Azufres, Mexico, as traced by noble gas isotopes, $\delta^{18}O$, δD, $\delta^{13}C$ and $^{87}Sr/^{86}Sr$. J. Volcanol. Geother. Res. 249, 1-11. https://doi.org/10.1016/j.jvolgeores.2012.09.006

Poblete Gonzales, C.P., Grelet, T., Tardani, D., Pinti, D.L., Sánchez, P., Álvarez-Amado, F., Tassara, S., Robidoux, P., Pérez-Flores, P., Aron, F., Berlo, K., Taussi, M., 2025. Volcano-tectonic control on magma residence time in arc crusts: Insights from noble gas geochemistry in the Andean Southern Volcanic Zone. 10.1016/j.epsl.2025.119426

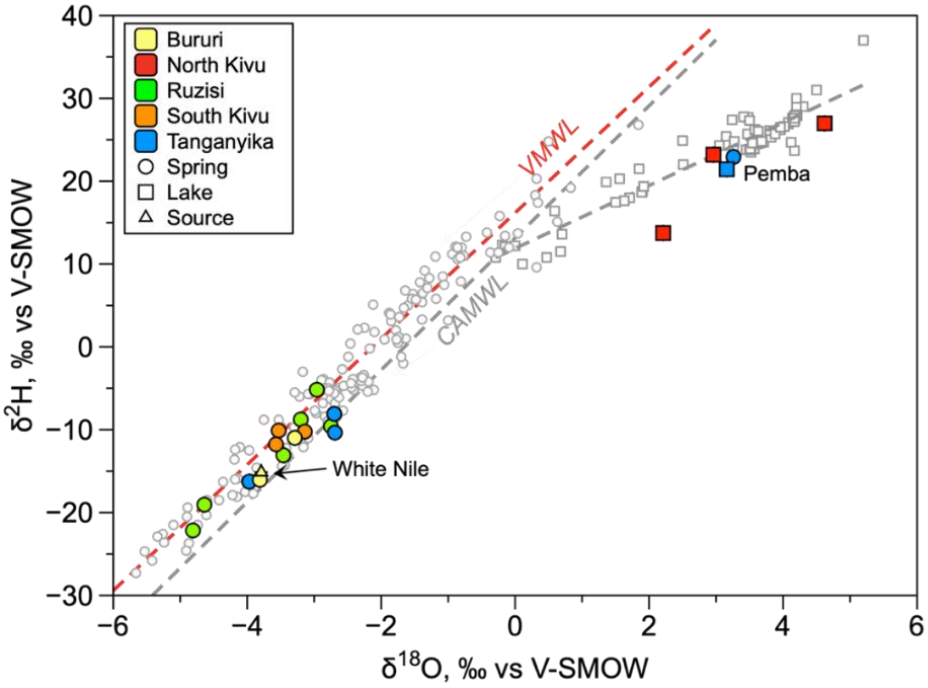
Pouclet, A., Bellon, H., & Bram, K. (2016). The Cenozoic volcanism in the Kivu rift : Assessment of the tectonic setting, geochemistry, and geochronology of the volcanic activity in the South-Kivu and Virunga regions. Journal of African Earth Sciences, 121, 219-246. https://doi.org/10.1016/j.jafrearsci.2016.05.026

Roulleau, E., Pinti, D.L., Famin, V., Bénard, B., Vinet, N., Bulot, A., d'Angelo, C., Claudon, M., Gambiez, J., Bouche, N., 2025. Geothermal resources of Réunion Island, Indian Ocean, studied by noble gas systematics in thermal springs. J. Volcanol. Geother. Res. 459, 108260. https://doi.org/10.1016/j.jvolgeores.2024.108260

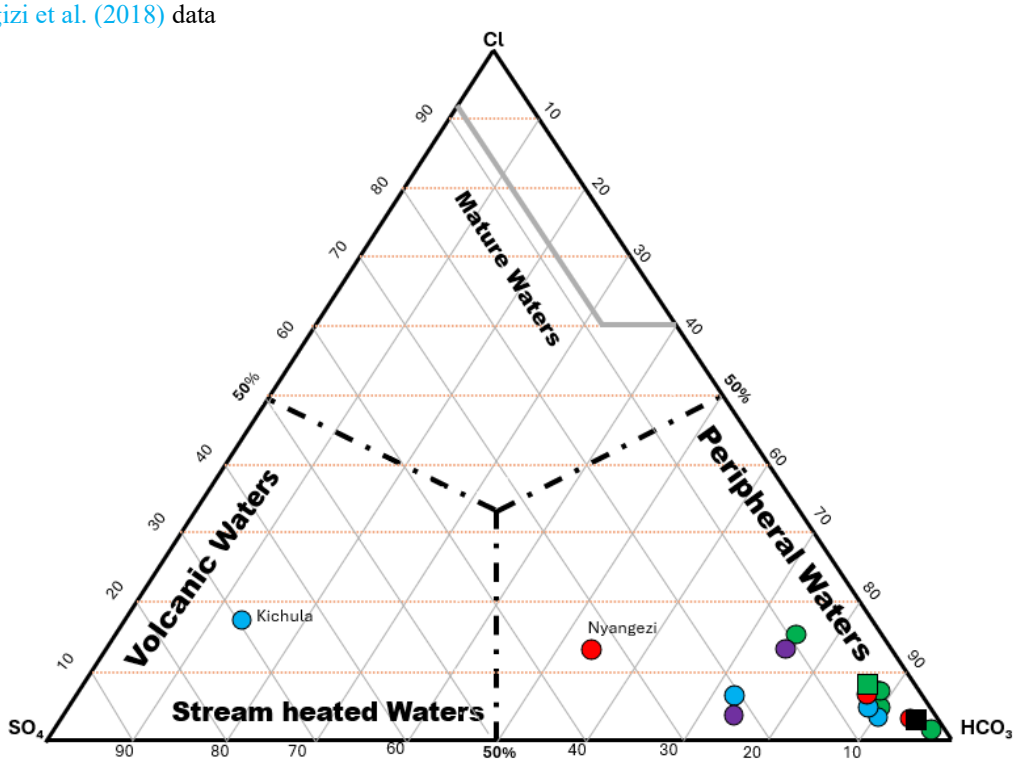
Smith, S.P., Kennedy, B.M., 1983. The solubility of noble gases in water and NaCl brine. Geochim. Cosmochim. Acta 47, 503-515.

Tedesco, D., Tassi, F., Vaselli, O., Poreda, R. J., Darrah, T., Cuoco, E., & Yalire, M. M. (2010). Gas isotopic signatures (He, C, and Ar) in the Lake Kivu region (western branch of the East African rift system) : Geodynamic and volcanological implications. Journal of Geophysical Research: Solid Earth, 115(B1), 2008JB006227. https://doi.org/10.1029/2008JB006227

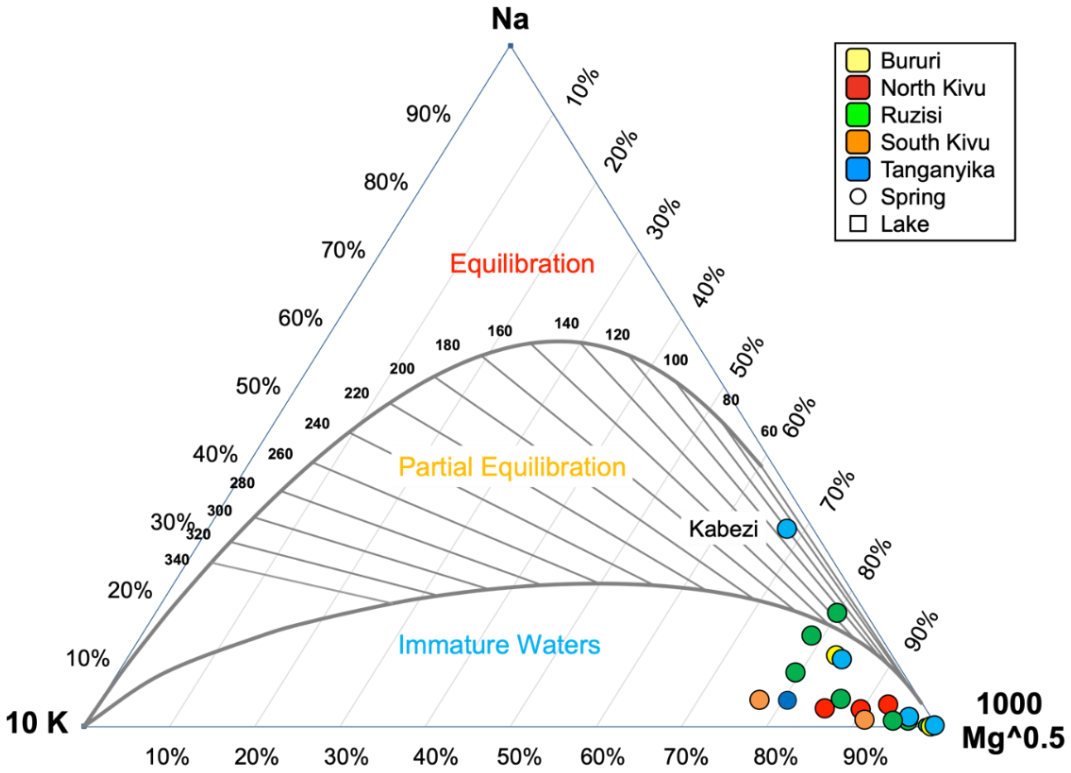
Torgersen, T., Drenkard, S., Stute, M., Schlosser, P., & Shapiro, A. (1995). Mantle helium in ground waters of eastern North America : Time and space constraints on sources. Geology, 23(8), 675.



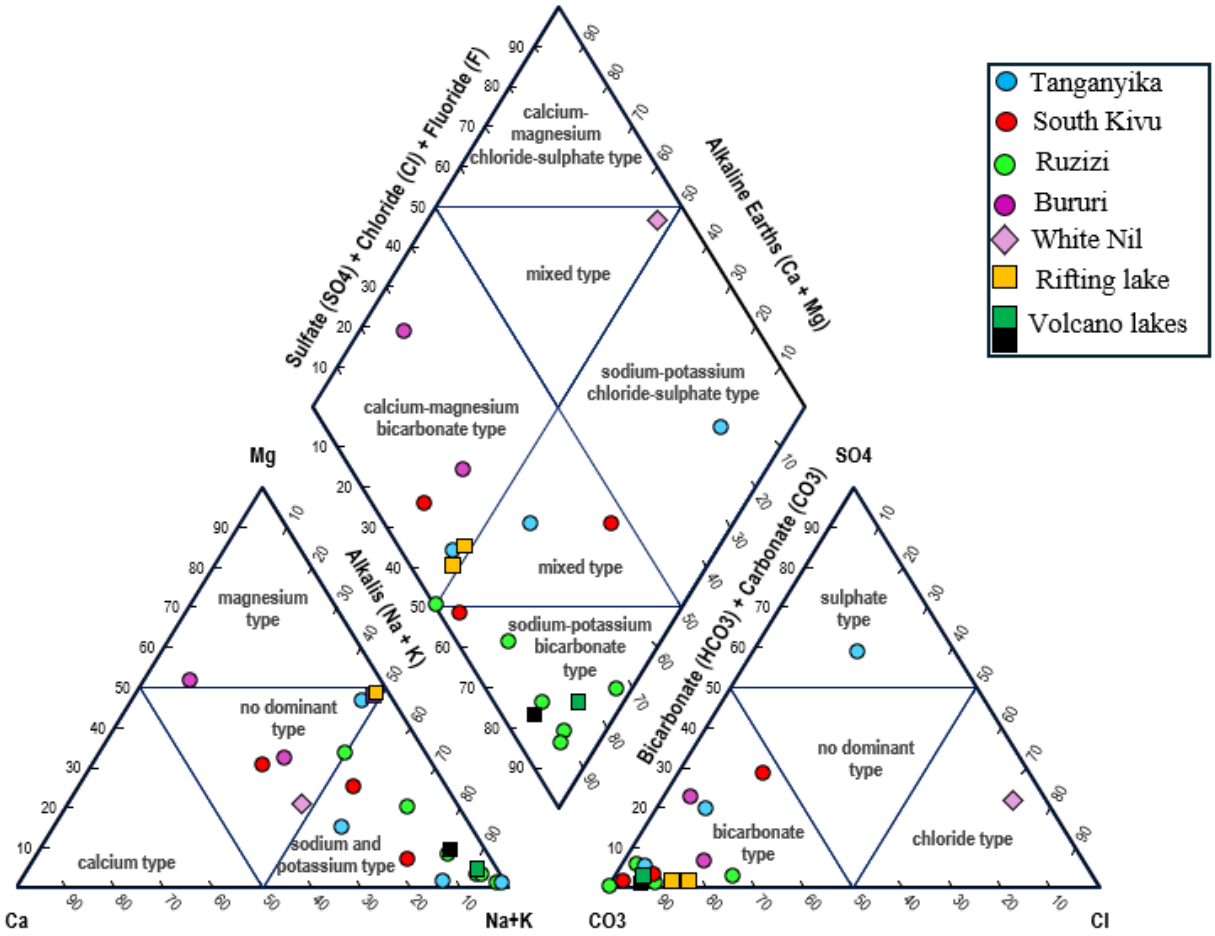
Annex 1. The δ^2H vs $\delta^{18}O$ plot for thermal spring, White Nile source and Kivu, Tanganyika, Lac Noir and Lac Vert Lake waters (this study). Small gray squares are literature data for WBERAS lakes Albert, Edwards, Kivu, Tanganyika and Malawi (Jasechko et al., 2013; Balagizi et al., 2018) while grey dots are local rainfall from Balagizi et al. (2018). The Virunga Meteoric Water Line (VMWL) and the Central Africa Meteoric Water Line (CAMWL) are also calculated from Balagizi et al. (2018) data



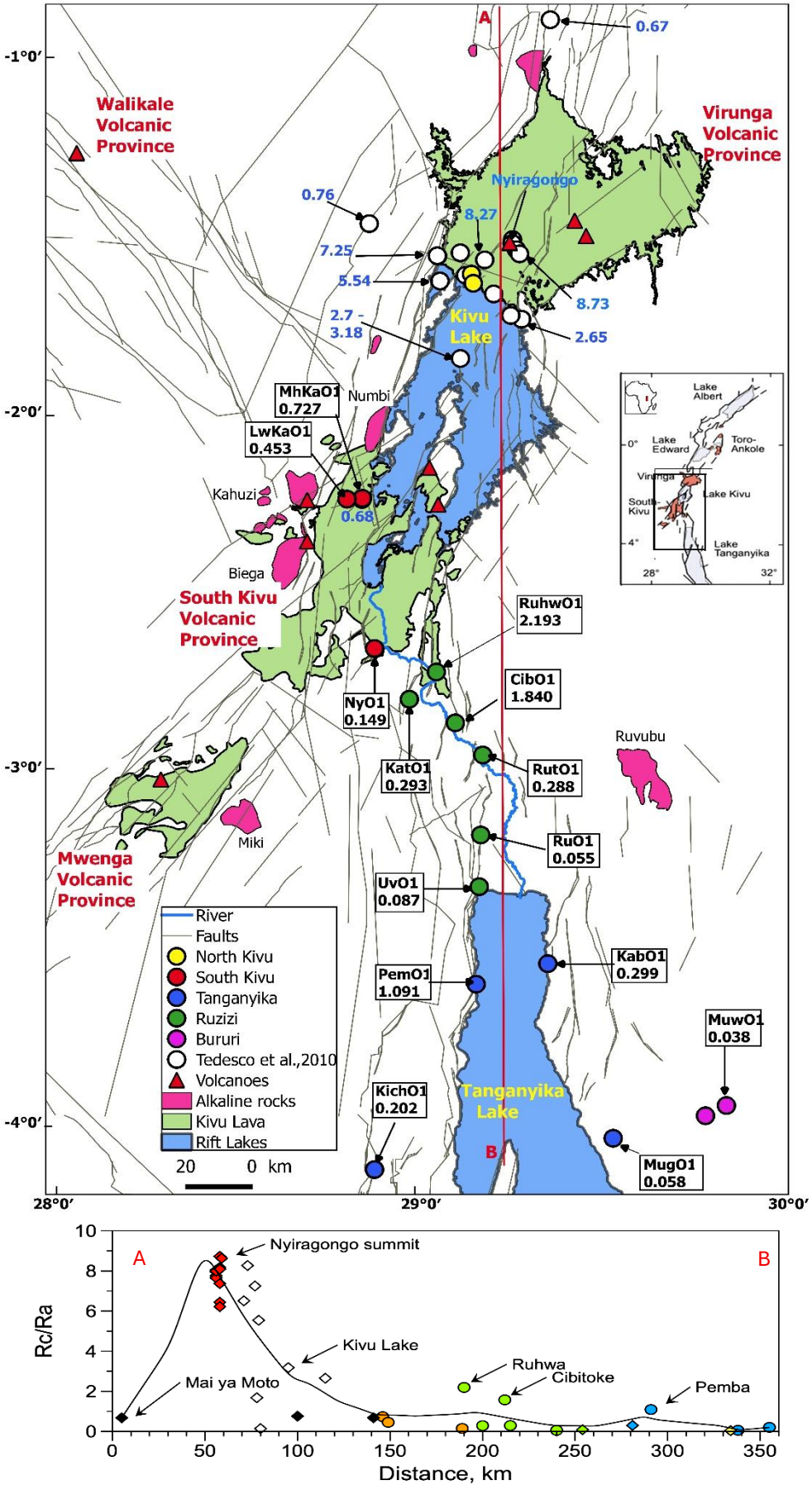
Annex 2. Ternary plot Cl - SO_4 - HCO_3 (Giggenbach and Goguel, 1989) of the sampled spring waters.



Annex 3. The Na-K-Mg diagram of Giggenbach (1998), which illustrates the degree of maturity of waters, represents the equilibrium between the dissolved Na-K-Mg in water and a mineral system.



Annex 4. Piper diagram of the sampled waters



Annex 5. Location of the study area with sampled springs and measured Rc/Ra values (this study; Tedesco et al., 2010). The bold red line is the cross-section of the 3D block in Figure 2. Figure from Pouclet et al. (2016), modified and redrawn.